Inorg. Chem. **2002**, *41*, 1492–1501

Formation of Double Cubanes $[Sn_7(NR)_8]$ in the Reactions of Pyridyl and Pyrimidinyl Amines with $Sn(NMe_2)_2$: A Synthetic and Theoretical Study†

David R. Armstrong,‡ Francesca Benevelli,§ Andrew D. Bond,§ Neil Feeder,§ Eilis A. Harron,§ Alexander D. Hopkins,§ Mary McPartlin,|| David Moncrieff,*,⊥ David Sáez,§ Elsje A. Quadrelli,§ Anthony D. Woods,§ and Dominic S. Wright*,§

Department of Pure and Applied Chemistry, University of Strathclyde, 195 Cathedral Street, Glasgow G1 1XL, U.K., Chemistry Department, University of Cambridge, Lensfield Road, Cambridge CB2 1EW, U.K., School of Chemistry, University of North London, London N7 8DB, U.K., and School of Computational Science Information and Technology, Florida State University, Tallahassee, Florida 32306

Received October 22, 2001

In contrast to the reactions of $Sn(NMe_2)_2$ with unfunctionalized primary amines (RNH_2), which yield the simple imido Sn^{II} cubanes $[SnNR]_4$, the reactions of 2-pyridyl or 2-pyrimidinyl amines give the mixed-oxidation-state Sn^{II}/Sn^{IV} double cubanes $[Sn_7(NR)_8]$. In addition to $[Sn_7\{2\text{-}N(5\text{-}Mepy)\}_8]\cdot 2thf$ (**1**·2thf) (py = pyridine) and $[Sn_7\{2\text{-}N(pm)\}_8]\cdot 0.33thf$ (**2**·0.33thf) (pm = pyrimidine), which were communicated previously, the syntheses and structures of the new complexes $[Sn_7\{2\text{-}N(4\text{-}Mepm)\}_8]\cdot 2thf$ (**3**·2thf), $[Sn_7\{2\text{-}N(4,6\text{-}Me_2pm)\}_8]\cdot 4thf$ (**4**·4thf), $[Sn_7\{2\text{-}N(4\text{-}Me\text{-}6\text{-}MeO\text{-}pm)\}_8]$ (**5**), and $[Sn_7\{2\text{-}N(4\text{-}MeO\text{-}6\text{-}MeO\text{-}pm)\}_8]$ (**6**) are reported. Model DFT calculations on the reactions of $Sn(NMe_2)_2$ with 2-$pmNH_2$ or $PhNH_2$, producing the cubanes $[Sn\{2\text{-}N(pm)\}]_4$ and $[SnNPh]_4$ (respectively), and the corresponding double cubanes $[Sn_7\{2\text{-}N(pm)\}_8]$ and $[Sn_7(NPh)_8]$, show that the presence of intramolecular Sn···N bonding which spans the cubane halves of the complexes is crucial to the formation of the double-cubane structure.

Introduction

Previous studies have shown that Sn^{II} imido cubanes of general formulas $[SnNR]_4$ are accessible using a variety of synthetic strategies. In certain cases nucleophilic substitution of $SnCl_2$[1] or $SnCp_2$[2] with RN^{2-} or RNH^- can be employed. However, acid−base reactions of the Sn^{II} reagents $[\{Me_2Si(NMe)_2\}Sn]$,[3] $[Sn\{N(SiMe_3)_2\}_2]$[4] and $[Sn(NMe_2)_2]$[5] with primary amines (RNH_2), hydrazines (H_2NNR_2), and borylamines (R_2BNH_2) provide more general approaches to these species. Of particular interest to us have been reactions which involve the base $[Sn(NMe_2)_2]$ since they have the advantage that they give clean formation of the cubanes for a broad range of amines at low temperatures.[5]

We have recently embarked on a research program involving the synthesis of functionalized cubanes $[SnNR]_4$, possessing O and N donor groups within their organic substituents (R).[6,7] Our primary aim was to investigate the use of these species as novel, three-dimensional Lewis bases for the assembly of a range of heterometallic molecular and extended arrangements. The previous studies noted above[1−5] led us to believe that little or no structural or chemical

† Dedicated to Ron Snaith.

* Authors to whom correspondence should be addressed. D.M.: moncrieff@csit.fsu.edu; fax, (850) 644 0098. D.S.W.: dsw1000@cus.cam.ac.uk; fax, +44 1223 336362.

‡ University of Strathclyde.

§ University of Cambridge.

|| University of North London.

⊥ Florida State University.

(1) Grigsby, W. J.; Hascall, T.; Ellison, J. J.; Olmstead M. M.; Power, P. P. *Inorg. Chem.* **1996**, *35*, 3254.

(2) Allan, R. E.; Beswick, M. A.; Davies, M. K.; Raithby, P. R.; Steiner A.; Wright, D. S. *J. Organomet. Chem.* **1998**, *550*, 71.

(3) (a) Veith, M.; Grosser, M. *Z. Naturforsch.* **1982**, *37B*, 1375. Veith, M.; Recktenwald, O. *Z. Naturforsch.* **1983**, *38B*, 1054. (b) Veith, M.; Schlemmer, G. *Chem. Ber.* **1982**, *115*, 2141.

(4) Chen, H.; Bartlett, R. A.; Dias, H. V. R.; Olmstead, M. M.; Power, P. P. *Inorg. Chem.* **1991**, *30*, 3390.

(5) Beswick, M. A.; Allen, R. E.; Paver, M. A.; Raithby, P. R.; Rennie, M.-A.; Wright, D. S. *J. Chem. Soc., Dalton Trans.* **1995**, 1991.

(6) Bashall, A.; Feeder, N.; Harron, E. A.; McPartlin, M.; Mosquera, M. E. G. *J. Chem. Soc., Dalton Trans.* **2000**, 4104.

(7) Benevelli, F.; Doyle, E. M.; Harron, E. A.; Feeder, N.; Quadrelli, E. A.; Sáez, D.; Wright, D. S. *Angew. Chem.* **2000**, *112*, 1559; *Angew. Chem., Int. Ed.* **2000**, *39*, 1501.

10.1021/ic011090r CCC: $22.00
Published on Web 02/22/2002

variations would occur in these species. However, our preliminary work on 2-amino-5-methylpyridine (2-NH_2-5-Mepy) and the related 2-aminopyrimidine (2-NH_2pm) revealed that unprecedented, mixed-oxidation-state Sn^{II}/Sn^{IV} double cubanes $[Sn_7(2\text{-}NR)_8]$ [R = 5-Mepy (**1**), pm (**2**)] are formed (py = pyridine, pm = pyrimidine).[7] One of the key factors governing the formation of **1** and **2** appears to be the way in which the heterocyclic ligands present affect the Sn^{II}/Sn^{IV} oxidation/reduction potential. Cyclic voltammetry (CV) of the discrete cubanes $[SnN^tBu]_4$ and $[SnNPh]_4$ suggests that the viability of the oxidation of Sn^{II} to Sn^{IV} in these species is highly influenced by the ligand present. The irreversible oxidation in $[SnN^tBu]_4$ at +1.00 V (vs Fe/Fe^{2+}) shifts to a more favorable value of +0.63 V in $[SnNPh]_4$. One suggestion is that the formation of the double cubane may occur via disproportionation of the cubane. A second factor pinpointed by the X-ray structural studies of **1** and **2** is the presence of Sn···N bonding between the heteroatoms of the 5-Mepy and pm groups. These interactions span the cubane halves of both complexes, therefore reinforcing the stability of this structure. Preliminary AM1 semiempirical calculations of the cubane $[Sn(2\text{-}Npy)]_4$ showed that these interactions are significant with respect to the core Sn−N bonding (the bond orders being about a quarter of the values for the core Sn−N bonds). However, the maintenance of a cubane structure for $[SnNCH_2(2\text{-}py)]_4$,[5] containing intramolecular Sn···N interactions similar to those of **1** and **2**, suggests that the formation of double cubanes may occur only in cases where the heterocyclic substituent is directly bonded to the imido-N center.

We present here a full account of this work. In addition to the structures of **1** and **2** (details of which were the subject of an earlier communication[7]), we report the structures of four other double-cubane derivatives $[Sn_7(2\text{-}NR)_8]$ [R = 4-Me-pyrimidine (4-Mepm) (**3**·2thf), 4,6-Me_2-pyrimidine (4,6-Me_2pm) (**4**·4thf), 4-Me-6-MeO-pyrimidine (4-Me-6-MeOpm) (**5**), and 4,6-$(MeO)_2$-pyrimidine (**6**) (4-MeO-6-MeOpm)] which not only illustrate the generality of this reaction but also allow an examination of the way in which the supramolecular structures of these complexes in the solid state are modified by ligand substitution. We also report model DFT calculations on the reactions of $Sn(NMe_2)_2$ with 2-pmNH_2 and PhNH_2, producing the cubanes $[Sn\{2\text{-}N(pm)\}]_4$ and $[SnNPh]_4$ (respectively) or the corresponding double cubanes $[Sn_7\{2\text{-}N(pm)\}_8]$ and $[Sn_7(NPh)_8]$. These show that the presence of intramolecular Sn···N bonding is crucial to the formation of the double-cubane structure.

Experimental and Calculational Section

Computational Details. Single-point, optimization, and frequency calculations were carried out using the Gaussian 98 (G98) software program.[8] All calculations were performed at the density functional theory (DFT) level[9] using the B3LYP functional.[10] The SSD basis set defined in the G98 program was initially used to make preliminary calculations on the cubane and double-cubane structures. The SSD basis set consists of an effective core potential (ECP), which represents 23 pairs of core electrons, augmented with a double-ζ sp basis set to represent the valence electrons on the Sn atom.[11] A Dunning 9s5p basis set[12] was used on all other atomic components as defined in the SSD basis. Single-point calculations were performed using an extended SSD basis set, which was created by addition of diffuse s and p functions on Sn using a common exponent of 0.0231[13] and a d function with an exponent of 0.18.[13] Diffuse and polarization functions were added to the carbon and nitrogen 9s5p basis set, designated D95++(d) within the G98 program, while a set of diffuse functions were appended to the hydrogen basis set utilizing the basis designated D95++ in G98. This extended SSD basis will be known as SSD-L in future references within this paper. The largest Sn basis set used in this series of calculations incorporated the SDB-cc-pVTZ basis[14] obtained from the EMSL Basis Set Library[15] and cc-pVDZ basis[16] for carbon, nitrogen, and hydrogen. This basis set combination will be designated as SDB throughout this paper. In all the basis sets specified, spherical harmonics were used throughout.

Two functional R groups were investigated in the cubane and double-cubane structures at the DFT level. One R group consisted of the phenyl (C_6H_5) fragment and the other the 2-pyrimidinyl ($C_4H_3N_2$) fragment. Geometry optimizations were performed using SSD and SDB basis sets while single-point calculations were performed using the SSD-L basis set. In preliminary studies on the double-cubane structure, no symmetry constraints were imposed in the geometry optimization process. The resultant optimized geometry was so close to the symmetry structure found through the use of the C_i point group that all subsequent calculations on the double-cubane structures retained C_i symmetry.

General Experimental Details. The compounds prepared in this study, $[Sn_7\{2\text{-}N(5\text{-}Mepy)\}_8]$·2thf (**1**·2thf), $[Sn_7\{2\text{-}N(pm)\}_8]$·0.33thf (**2**·0.33thf), $[Sn_7\{2\text{-}N(4\text{-}Mepm)\}_8]$·2thf (**3**·2thf), $[Sn_7\{2\text{-}N(4,6\text{-}Me_2\text{-}pm)\}_8]$·4thf (**4**·4thf), $[Sn_7\{2\text{-}N(4\text{-}Me\text{-}6\text{-}MeO\text{-}pm)\}_8]$ (**5**), and $[Sn_7$-

(8) Frisch, M. J.; Trucks, G. W.; Schlegel, H. B.; Scuseria, G. E.; Robb, M. A.; Cheeseman, J. R.; Zakrzewski, V. G.; Montgomery, J. A., Jr.; Stratmann, R. E.; Burant, J. C.; Dapprich, S.; Millam, J. M.; Daniels, A. D.; Kudin, K. N.; Strain, M. C.; Farkas, O.; Tomasi, J.; Barone, V.; Cossi, M.; Cammi, R.; Mennucci, B.; Pomelli, C.; Adamo, C.; Clifford, S.; Ochterski, J.; Petersson, G. A.; Ayala, P. Y.; Cui, Q.; Morokuma, K.; Malick, D. K.; Rabuck, A. D.; Raghavachari, K.; Foresman, J. B.; Cioslowski, J.; Ortiz, J. V.; Baboul, A. G.; Stefanov, B. B.; Liu, G.; Liashenko, A.; Piskorz, P.; Komaromi, I.; Gomperts, R.; Martin, R. L.; Fox, D. J.; Keith, T.; Al-Laham, M. A.; Peng, C. Y.; Nanayakkara, A.; Challacombe, M.; Gill, P. M. W.; Johnson, B.; Chen, W.; Wong, M. W.; Andres, J. L.; Gonzalez, C.; Head-Gordon, M.; Replogle, E. S.; Pople, J. A. *Gaussian 98*, revision A.9; Gaussian, Inc.,: Pittsburgh, PA, 1998.

(9) (a) Hohenberg, P.; Kohn, W. *Phys. Rev.* **1964**, *136*, B864. (b) Kohn, W.; Sham, L. J. *Phys. Rev.* **1965**, *140*, A1133.

(10) Becke, A. D. *J. Chem. Phys.* **1993**, *104*, 1040.

(11) Kuechle, W.; Dolg, M.; Stoll, H.; Preuss, H. *Mol. Phys.* **1991** *74*, 1245. Stuttgart Relativistic, Large Core ECP Basis Set.

(12) Dunning, T. H., Jr.; Hay, P. J. In *Methods of Electronic Structure Theory*; Schaefer, H. F., III, Ed.; Plenum Press: New York, 1977; Vol. 3.

(13) GAMESS Reference Manual, pp 4−12 and references contained therein, 2001. http://www.msg.ameslab.gov/GAMESS/doc.menu.html.

(14) Basis set exponents and contractions were taken from Martin and Sundermann: Martin, J. M. L.; Sundermann, A. *J. Chem. Phys.* **2001**, *114*, 3408. Relativistic ECP definitions were taken fromBergner et al.: Bergner, A.; Dolg, M.; Kuechle, W.; Stoll, H.; Preuss, H. *Mol. Phys.* **1993**, *80*, 1431.

(15) Basis sets were obtained from the Extensible Computational Chemistry Environment Basis Set Database, Version 8/01/01, as developed and distributed by the Molecular Science Computing Facility, Environmental and Molecular Sciences Laboratory which is part of the Pacific Northwest Laboratory, P.O. Box 999, Richland, WA 99352, and funded by the U.S. Department of Energy. The Pacific Northwest Laboratory is a multiprogram laboratory operated by Battelle Memorial Institue for the U.S. Department of Energy under Contract DE-AC06-76RLO 1830. Contact David Feller or Karen Schuchardt for further information. http://www.emsl.pnl.gov:2080/forms/basisform.html.

(16) Dunning, T. H., Jr. *J. Chem. Phys.* **1989**, *90*, 1007.

{2-N(4-MeO-6-MeO-pm)}$_8$] (**6**), are air- and moisture-sensitive.[17] They were handled on a vacuum line using standard inert atmosphere techniques and under dry/oxygen-free argon. Toluene, Et_2O, and thf were dried by distillation over sodium/benzophenone prior to the reactions. The products were isolated and characterized with the aid of an argon-filled glovebox fitted with a Belle Technology O_2 and H_2O internal recirculation system. $Sn(NMe_2)_2$ was prepared using the literature procedure, from the reaction of $SnCl_2$ with a suspension of $LiNMe_2$ in Et_2O.[18] The pyridines and pyrimidines (used in the syntheses of **1**−**6**) were acquired from Aldrich and were used as supplied. Elemental analyses were performed by first sealing the samples under argon in airtight aluminum boats (1−2 mg) and then analyzing C, H, and N content using an Exeter Analytical CE−440 elemental analyzer. Proton NMR spectra were recorded on a Bruker WM 400 MHz spectrometer in dry deuterated DMSO (using the solvent resonances as the internal reference standard). The syntheses of **1** and **2** are reported in ref 7.

Synthesis of 3. A solution of 2-amino-4-methylpyrimidine in thf (15 mL) at −78 °C (0.44 g, 4.0 mmol) was added to a solution of $Sn(NMe_2)_2$ (0.83 g, 4.0 mmol) in thf (15 mL). The mixture was stirred (30 min) and allowed to warm to ca. 0 °C. Immediate storage at room temperature (12 h) gave light yellow cubes of **3**. Elemental analysis suggests that both of the lattice thf molecules are removed by placing samples of the complex under vacuum (10^{-1} atm, 15 min) during isolation. Yield: 0.17 g (19%). Dec: 246 °C. IR (Nujol, NaCl): ν_{max}/cm^{-1} 1662 (w), 1569 (s), 1543 (s), 1423 (s), 1350 (vs), 1311 (s), 1240 (s), 1169 (w), 1097 (m), 1039 (s), 984 (m), 944 (w). Elemental anal. Found: C 28.7, H 2.7, N 17.7. Calcd: C 28.4, H 2.4, N 19.9.

Synthesis of 4. A solution of 2-amino-4,6-dimethylpyrimidine (0.31 g, 2.5 mmol) in thf (35 mL) was added to a solution of $Sn(NMe_2)_2$ (0.52 g, 2.5 mmol) in thf (20 mL) at −78 °C. The mixture was stirred (30 min). The solution was stored at room temperature for 12 h. Colorless cubes of **4** were formed. Elemental analysis suggests that both of the lattice thf molecules are removed by placing samples of the complex under vacuum (10^{-1} atm, 15 min) during isolation. Yield: 0.15 g (26%). Dec: 222 °C. IR (Nujol, NaCl): ν_{max}/cm^{-1} 1621 (m), 1567 (s), 1354 (s), 1195 (vs), 1169 (w), 1149 (w), 967 (w), 859 (w), 792 (m), 773 (w). ^{1}H NMR (+25 °C, d_6-DMSO, 400.1 MHz): 6.51 (s, 8H, C−H on aromatic ring), 3.28 (s, 24H, Me). Elemental anal. Found: C 27.9, H 2.8, N 17.4. Calcd: C 33.3, H 3.1, N 18.7.

Synthesis of 5. A solution of 2-amino-4-methoxy-6-methylpyrimidine (0.59 g, 4.0 mmol) in toluene (20 mL) was added to a solution of $Sn(NMe_2)_2$ (0.83 g, 4.0 mmol) in toluene (10 mL) at −78 °C. The mixture was stirred (30 min) before being allowed to warm to room temperature. Reduction of the solvent under vacuum (to ca. 20 mL) and storage at room temperature (12 h) gave colorless cubes of **5**. Yield: 0.25 g (26%). Dec: 282 °C. IR (Nujol, NaCl): ν_{max}/cm^{-1} 1634 (w), 1378 (s), 1365 (s), 1338 (vs), 1261 (w), 1202 (w), 1156 (w), 1087 (w), 1044 (w). ^{1}H NMR (+25 °C, d_6-DMSO, 400.1 MHz): 6.07 (s, 8H, C−H on aromatic ring), 3.96 (s, 24H, MeO), 2.32 (s, 24H, Me). Elemental anal. Found: C 31.3, H 3.1, N 17.3. Calcd: C 29.9, H 2.9, N 17.4.

Synthesis of 6. A solution of 2-amino-4,6-dimethoxypyrimidine (0.62 g, 4.0 mmol) in toluene (10 mL) was added to a solution of $Sn(NMe_2)_2$ (0.83 g, 4.0 mmol) in toluene (20 mL) at −78 °C. The reaction mixture was stirred at this temperature (30 min) and was then allowed to warm to room temperature, where it was stirred further (30 min). A pale yellow solution was produced. The solvent was reduced under vacuum by ca. 5 mL, and storage at room temperature (12 h) gave a crop of colorless crystals of **6**. Yield: 0.08 g (8%). Dec: 215 °C (black solid formed by 340 °C). IR (Nujol, NaCl): ν_{max}/cm^{-1} 1377 (s), 1326 (vs), 1261 (w), 1248 (w), 1209 (m), 1193 (m), 1156 (m), 1106 (m), 1077 (m), 1014 (w). ^{1}H NMR (+25 °C, d_6-DMSO, 400.1 MHz): 5.31 (s, 8H, aromatic C−H), 3.28 (s, 18H, *endo*-MeO), 3.26 (s, 30H, *exo*-MeO and terminal 4,6-$(MeO)_2$pm ligands). Elemental anal. Found: C 28.1, H 2.9, N 15.3. Calcd: C 28.0, H 2.7, N 16.4.

Scheme 1

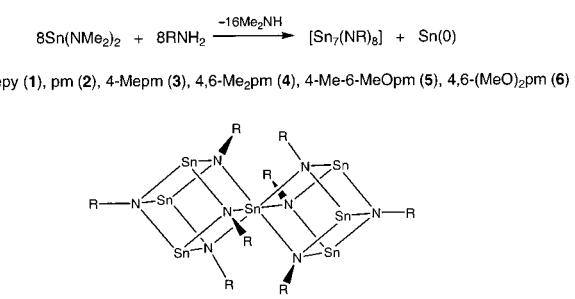

Solid-State MAS-NMR. ^{119}Sn solid-state NMR spectra were acquired at 148.99 MHz with a Chemagnetics CMX 400 spectrometer and a commercial MAS probehead with zirconium rotors 4 mm in diameter. The half-pulse length was 2.0 μs, the recycle delay 120 s, and the spinning speed 8 kHz. Solid $SnCl_2$ was used as the external standard,

X-ray Crystallographic Studies of 1−6. Crystals of **1**−**6** were mounted directly from solution under argon using an inert oil which protects them from atmospheric oxygen and moisture.[19] X-ray intensity data for **1**−**5** were collected using a Nonius Kappa CCD diffractometer, and that for **6** using a Siemens P4 four-circle diffractometer. The structures were solved by direct methods and refined by full-matrix least squares on F^2.[20] The two thf molecules per molecule present in the lattice of **3** and the four molecules present in the lattice of **4** were not disordered. Atomic coordinates, bond lengths and angles, and thermal parameters for **1**−**6** have been deposited with the Cambridge Crystallographic Data Center.

Results and Discussion

Complexes **1**−**6** were prepared by the 1:1 reactions of the appropriate aminopyridines and -pyrimidines with [$Sn(NMe_2)_2$] in thf or toluene (Scheme 1). The reactions producing **1**−**6** have similar characteristics. If the reagents in solution are stirred at room temperature or above, precipitation of the products occurs, with the powders formed being only sparingly soluble in most organic solvents. The best method of obtaining pure, crystalline samples of compounds **1**−**3** was found to be performing the reactions at ca. −78 °C and allowing the temperature to rise slowly to ca. 0 °C. At this point immediate prolonged storage of the solutions at room temperature gave crystalline samples of each. However, complexes **4**−**6**, containing disubstituted pyrimidine ligands, are more soluble. In particular, both **5** and **6** are synthesized in toluene rather than thf as the solvent, and **6** can be heated back into solution once precipitation of

(17) Shriver, D. F.; Drezdon, M. A. *'The Manipulation of Air-Sensitive Compounds*, 2nd ed.; Wiley: New York, 1986.
(18) Olmstead, M. M.; Power, P. P. *Inorg. Chem.* **1984**, *23*, 413.
(19) Kottke, T.; Stalke, D. *J. Appl. Crystallogr.* **1993**, *26*, 615.
(20) Sheldrick, G. M. *SHELXTL*, PC version 5.03; Siemens Analytical Instruments: Madison, WI, 1994.

Table 1. Crystal Data and Refinements for $[Sn_7\{2\text{-}N(4\text{-}Mepm)\}_8]\cdot 2thf$ (**3**·2thf) $[Sn_7\{2\text{-}N(4,6\text{-}Me_2pm)\}_8]\cdot 2thf$ (**4**·4thf), $Sn_7\{2\text{-}N(4\text{-}Me\text{-}6\text{-}MeO\text{-}Me_2pm)\}_8]$ (**5**), and $[Sn_7\{2\text{-}N(4,6\text{-}(MeO)_2\text{-}Me_2pm)\}_8]$ (**6**)

	3·2thf	**4**·4thf	**5**	**6**
fw	1832.00	2088.41	1928.00	2056.00
T (K)	180(2)	200(2)	180(2)	198(2)
cryst syst	triclinic	triclinic	triclinic	triclinic
space group	$P\bar{1}$	$P\bar{1}$	$P\bar{1}$	$P\bar{1}$
a (Å)	10.9902(6)	12.1860(4)	11,483(2)	12.779(6)
b (Å)	11.6813(5)	12.7060(8)	11.773(2)	12.754(7)
c (Å)	13.2627(9)	12.9930(8)	12.155(2)	13.155(5)
α (deg)	71.761(3)	83.066(2)	86.620(10)	91.91(3)
β (deg)	73.956(3)	81.957(3)	84.690(10)	115.07(2)
γ (deg)	68.437(3)	75.450(3)	80.740(10)	117.10(4)
V (Å^3)	1478.63(14)	1920.40(18)	1556.09(15)	1659.3(13)
Z	1	1	1	1
D_{calcd} (Mg·m^{-3})	2.057	1.806	1.985	2.057
μ (Mo Kα) (mm^{-1})	2.968	2.300	2.733	2.673
R indices[a] [$I>2\sigma(I)$]	R1 = 0.040, wR2 = 0.077	R1 = 0.049, wR2 = 0.116	R1 = 0.052, wR2 = 0.111	R1 = 0.031, wR2 = 0.052
R indices (all data)	R1 = 0.074, wR2 = 0.101	R1 = 0.075, wR2 = 0.128	R1 = 0.083, wR2 = 0.135	R1 = 0.053, wR2 = 0.064

[a] $R1 = \sum||F_o| - |F_c||/\sum|F_o|$. $wR2 = |\sum w(F_o^2 - F_c^2)^2/\sum(F_o^2)^2]^{1/2}$. $w = 1/[\sigma(F_o)^2 + P(F_o^2 + 3F_c^2)/3]$.

the complex has occurred. ^{1}H and ^{119}Sn NMR spectroscopic studies of **1**−**3** were hampered by the low solubilities of these materials and their extremely hygroscopic nature. After attempts to heat crystalline samples into DMSO, all gave ^{1}H NMR spectra characteristic of the amines themselves (RNH_2) rather than the imido groups (RN^{2-}). We assume that this is the result of trace hydrolysis and the far greater solubility of the amines than the complexes in solution. The greater solubilities of complexes **4**, **5**, and **6** in DMSO allowed the ^{1}H NMR spectra of the complexes to be obtained, although only in the case of the most soluble complex **6** could a satisfactory ^{119}Sn NMR spectrum be recorded. Interestingly, two closely separated MeO resonances are observed in the ^{1}H NMR spectrum of **6** [δ = 3.28 (s, 30H) and 3.26 (s, 18H)]. The presence of two resonances suggests that there is restricted rotation about the imido-N−C bonds for the six 4,6-$(MeO)_2$pm ligands which span the two cubane subunits of the Sn_7N_8 core of the complex. Thus the *endo*-4-MeO groups [facing toward the Sn^{IV} center] are rendered magnetically distinct from the *exo*-6-MeO groups (18H), with the *exo*-MeO resonance (18H) being coincident with that for 4- and 6-MeO groups of the terminal 4,6-$(MeO)_2$pm ligands (12H).

The IR spectra of **1**−**6** reveal that no N−H protons remain in the products. This, combined with the solid-state ^{119}Sn MAS-NMR spectra of **2**, **3**, and **4** which showed the presence of Sn^{II} and Sn^{IV}, confirmed the formulation of **2**−**4** as the mixed-oxidation-state species $[Sn_7(NR)_8]$ rather than the possible alternative Sn^{II} species $[Sn_7(NR)_8H_2]$ (in which two of the ligands are protonated). In the solid-state NMR spectrum of **2** (containing the unsubstituted pyrimidine ligand), the Sn^{IV} and Sn^{II} resonances are found at δ 353.7 and −180.4, respectively. The incorporation of Me substituents into the 4- and 6-positions of the pyrimidine framework results in a marked shift toward more positive values for the Sn^{IV} resonance (δ 423.2 in **3** and 472.8 in **4**) and a large shift toward more negative values for the Sn^{II} centers (δ −942.8 in **3** and −996.2 in **4**). As noted above, the reasonably high solubility of **6** in DMSO allowed solution ^{119}Sn NMR investigations to be undertaken. The solution ^{119}Sn NMR spectrum of the complex again confirms the presence of Sn^{II} (δ −284.8) and Sn^{IV} (δ 75.4). The formulation of **1**−**6** as mixed-oxidation-state complexes was later confirmed by their X-ray structures. It should be noted that although **1**−**4** crystallize as thf solvates, elemental analysis reveals that the lattice-bound thf molecules present are removed when crystalline samples are placed under vacuum during isolation (ca. 15 min, 10^{-1} atm).

The low-temperature (180−198 K) X-ray structures of **1**−**6** were obtained. Since the structures of **1** and **2** were reported by us in an earlier communication,[7] it will not be appropriate to discuss them further here except by comparison with the structurally related complexes **3**−**6**, and in relation to their supramolecular association in the solid state

Table 2. Selected Bond Lengths (Å) and Angles (deg) for the Double Cubanes $[Sn_7\{2\text{-}N(4\text{-}Mepm)\}_8]\cdot 2thf$ (**3**·2thf), $[Sn_7\{2\text{-}N(4,6\text{-}Me_2pm)\}_8]\cdot 2thf$ (**4**·4thf), $Sn_7\{2\text{-}N(4\text{-}Me\text{-}6\text{-}MeO\text{-}Me_2pm)\}_8]$ (**5**), and $[Sn_7\{2\text{-}N(4,6\text{-}(MeO)_2\text{-}Me_2pm)\}_8]$ (**6**)

	3·2thf	**4**·4thf	**5**	**6**
		Bond Lengths (Å)		
Sn(1)−N(1)	2.153(3)	2.161(5)	2.141(9)	2.145(5)
Sn(1)−N(5)	2.168(4)	2.164(6)	2.151(9)	2.160(5)
Sn(1)−N(7)	2.154(4)	2.149(5)	2.164(8)	2.155(5)
Sn(2)−N(3)	2.277(3)	2.263(6)	2.199(9)	2.214(5)
Sn(2)−N(5)	2.218(3)	2.181(5)	2.232(8)	2.248(5)
Sn(2)−N(7)	2.203(4)	2.241(6)	2.263(9)	2.227(5)
Sn(3)−N(1)	2.267(4)	2.211(6)	2.213(9)	2.240(5)
Sn(3)−N(3)	2.230(4)	2.216(5)	2.195(8)	2.286(5)
Sn(3)−N(5)	2.218(3)	2.285(6)	2.297(8)	2.214(5)
Sn(4)−N(1)	2.236(4)	2.320(5)	2.241(8)	2.246(5)
Sn(4)−N(3)	2.200(4)	2.230(6)	2.278(9)	2.198(5)
Sn(4)−N(7)	2.254(3)	2.213(5)	2.187(9)	2.322(5)
N(2,6,8)···Sn(2A,3A,4A)	2.812(4)−2.864(4)	3.161(5)−3.172(6)	2.990(5)−3.188(6)	2.838(5)−3.052(5)
		Angles (deg)		
N−Sn(2,3,4)−N	77.2(1)−80.3(1)	76.7(2)−80.5(2)	76.2(3)−80.5(3)	75.6(2)−80.8(2)
Sn−N(1,3,5,7)−Sn	97.4(1)−101.6(2)	98.4(2)−102.1(2)	98.0(4)−102.7(3)	98.0(2)−102.2(2)
N−Sn(1)−N[a]	80.1(1)−81.9(1)	80.2(1)−81.5(2)	80.5(3)−81.0(3)	80.2(2)−81.5(2)
N−Sn(1)−N[b]	98.1(1)−99.6(2)	98.5(2)−99.8(2)	99.0(3)−99.5(3)	98.5(2)−99.8(2)

[a] Inside each cubane. [b] Between cubanes.

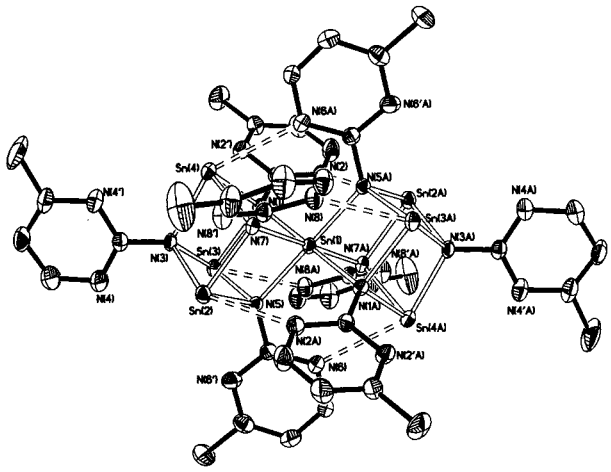

Figure 1. Structure of $[Sn_7\{2\text{-}N(4\text{-}Mepm)\}_8]\cdot 2thf$ (**3**·2thf). H atoms and lattice-bound thf molecules have been omitted for clarity. Thermal ellipsoids are drawn at the 40% probability level.

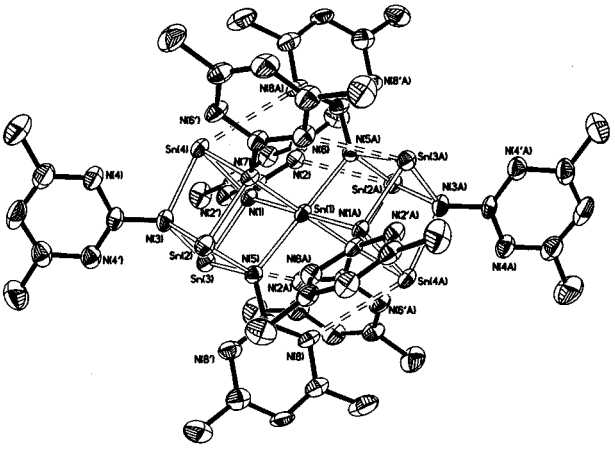

Figure 2. Structure of $[Sn_7\{2\text{-}N(4,6\text{-}Mepm)\}_8]\cdot 4thf$ (**4**·4thf). H atoms and lattice-bound thf molecules have been omitted for clarity. Thermal ellipsoids are drawn at the 40% probability level.

(which has not been discussed previously). Details of the data collections and structural refinements are given in Table 1. Table 2 lists key bond lengths and angles for **3**, **4**, **5**, and **6**.

The low-temperature structures of $[Sn_7\{2\text{-}N(4\text{-}Mepm)\}_8]\cdot 2thf$ (**3**·2thf) (Figure 1), $[Sn_7\{2\text{-}N(4,6\text{-}Me_2pm)\}_8]\cdot 4thf$ (**4**·4thf) (Figure 2), $[Sn_7\{2\text{-}N(4\text{-}Me\text{-}6\text{-}MeO\text{-}pm)\}_8]$ (**5**) (Figure 3), and $[Sn_7\{2\text{-}N(4\text{-}MeO\text{-}6\text{-}MeO\text{-}pm)\}_8]$ (**6**) (Figure 4) are similar to those of $[Sn_7(2\text{-}NR)_8]$ [R = 5-Mepy (**1**), pm (**2**)].[7] All of these complexes are centrosymmetric cages composed of two Sn_4N_4 cubanes which share a central Sn^{IV} atom, located at the crystallographic center of symmetry. Complexes **3** and **4** crystallize with two and four molecules of thf in the lattices, respectively. Although double-cubane arrangements have been observed for a range of main group and transition metal complexes, they have only been found previously for species containing alkoxide, sulfide, or halide bridges.[21] The double-cubane arrangement observed for **1**−**6** represents a new structural class of Sn^{II} imido complexes.[22] This structural motif can be viewed alternatively as composed of central Sn^{4+} cations which are coordinated by two tripodal $[Sn_3(NR)_4]^{2-}$ dianions. Anions of this type have been

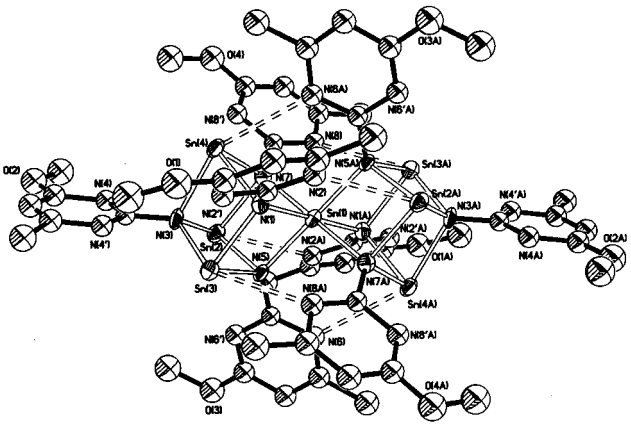

Figure 3. Structure of $[Sn_7\{2\text{-}N(4\text{-}Me\text{-}6\text{-}MeOpm)\}_8]$ (**5**). H atoms have been omitted for clarity. Thermal ellipsoids are drawn at the 40% probability level.

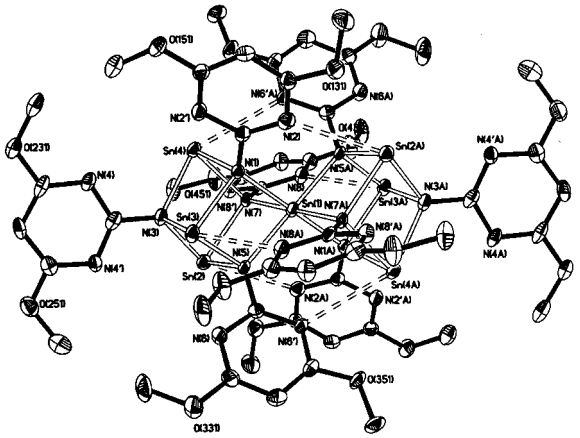

Figure 4. Structure of $[Sn_7\{2\text{-}N(4,6\text{-}(MeO)_2\text{-}Me_2pm)\}_8]$ (**6**). H atoms have been omitted for clarity. Thermal ellipsoids are drawn at the 40% probability level.

observed before in the salt $[^tBuNSn_3(Nnaph)_3Li]^-[Li(thf)_4]^+$ (naph = 1-naphthalene).[23]

The range of Sn−N bond lengths made with the Sn^{IV} centers in **3**−**6** [range Sn(1)−N 2.141(9)−2.168(4) Å] and the internal N−Sn−N angles at these centers within the cubane units [range 80.1(1)−81.9(1)°] are very similar to those found in **1** and **2** [with ranges of 2.157(3)−2.177(5) Å and 80.8(1)−82.6(2)°, respectively]. The compression of

(21) (a) Ziegler, M. L.; Weiss, J. *Angew. Chem.* **1970**, *83*, 931; *Angew. Chem., Int. Ed. Engl.* **1970**, *9*, 931. (b) Shibahara, T.; Yamamoto, T.; Kanadani, H.; Kuruya, H. *J. Am. Chem. Soc.* **1987**, *109*, 3495. (c) Swamy, K. C. K.; Day, R. O.; Holmes, R. R. *J. Am. Chem. Soc.* **1988**, *110*, 7543. (d) Skashi, A. H.; Shibahara, T. *Inorg. Chem.* **1989**, *28*, 2906. (e) Ishimori, M.; Hagiwara, T.; Tsuruta, T.; Yasuoka, N.; Kasai, N. *Bull. Chem. Soc. Jpn.* **1976**, *46*, 1165. (f) Hernandez-Molina, R.; Dybster, D. N.; Fedin, V. D.; Elsegood, M. R. J.; Clegg, W.; Sykes, S. G. *Inorg. Chem.* **1989**, *37*, 2995. (g) Clerk, M. D.; Zaworotko, M. J. *J. Chem. Soc., Chem. Commun.* **1991**, 1607. (h) Busching, I.; Strasdeit, H. *J. Chem. Soc., Chem. Commun.* **1994**, 2789. (i) Sakane, G.; Yao, Y.; Shibahara, T. *Inorg. Chim. Acta* **1994**, *13*, 216. (j) Herrmann, W. A.; Egli, A.; Herdtweck, A.; Alberto, R.; Baumgarten, F. *Angew. Chem.* **1996**, *108*, 486; *Angew. Chem., Int. Ed. Engl.* **1996**, *35*, 432.

(22) Although no other mixed-oxidation-state imido complexes of this type exist, there are examples of organometallic Sn(II)/Sn(IV) complexes, e.g.: Benet, S.; Cardin, C. J.; Cardin, D. J.; Constantine, S. P.; Heath, P.; Rashidi, H.; Teixeira, S.; Thorpe, J. H.; Todd, A. K. *Organometallics* **1999**, *18*, 389.

(23) Allan, R. E.; Beswick, M. A.; Paver, M. A.; Raithby, P. R.; Steiner, A.; Wright, D. S. *Chem. Commun. (Cambridge)* **1996**, 1501.

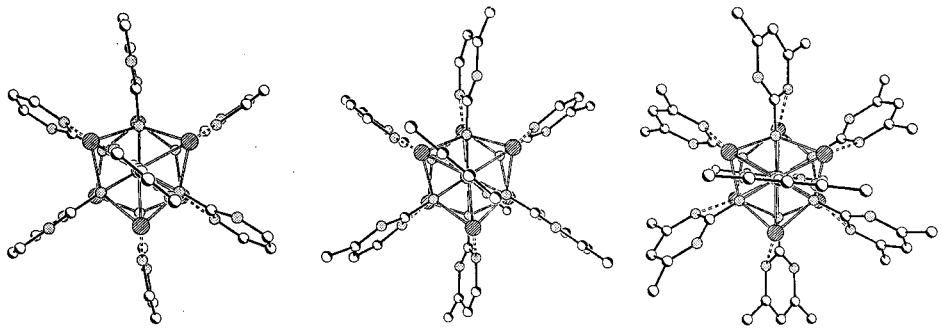

Figure 5. Comparison of the Sn···N interactions found in **2**, **3**, and **4** viewed down the major axis. The effect of Me substitution leading to misalignment of the donor-N centers.

the internal N−Sn−N angles at the Sn^{IV} centers in **1**−**6** (cf. ca. 99° for the N−Sn−N angles between the cubane units) results in distorted octahedral geometries which are akin to that occurring in the $[Sn(NHCy)_6]^{2-}$ dianion of [thf·Li(μ-NH)$_3$Sn(μ-NHCy)$_3$Li·thf].[24] The Sn−N bond lengths to the Sn(II) centers in **3**−**6** [range 2.218(3)−2.322(5) Å], the associated N−Sn−N angles [range 75.6(2)−80.8(2)°], and the Sn−N−Sn angles in all four complexes [range 97.2(1)−102.7(3)°] are all similar to those observed in **1** and **2**.[7] These parameters are comparable to those found in discrete cubanes of the type $[SnNR]_4$ [Sn−N range 2.15(1)−2.34(2) Å, N−Sn−N mean 81.9°, and Sn−N−Sn mean 98.4°].[1−5]

Another similarity between the structures of **3**−**6** and those of **1** and **2** is the presence of relatively short Sn···N interactions between the Sn^{II} centers of the cores and a N donor center of each of the pyridyl or pyrimidine N groups. These interactions span the two cubane halves of the molecules and may play a role in promoting the formation of the double-cubane structures of the complexes. Although the Sn···N interactions in **1**−**3** are similar [2.761(5)−2.784(5) Å in **1**, 2.807(3)−2.935(3) Å in **2**, and 2.812(4)−2.864(4) Å in **3**], Me and MeO substitution of the 4- and 6-positions of the pyimidine rings in **4** and **5** results in far longer intramolecular Sn···N contacts [range 3.161(5)−3.172(6) Å in **4** and 2.990(5)−3.188(6) Å in **5**; cf. ca. 3.70 Å estimated for van der Waals interaction[25]]. In **3**, it is the less sterically shielded ring-N centers (that are remote from the 4-Me substituent) which are involved in the Sn···N interactions, with the pyrimidine rings being aligned (as in the unsubstituted complex **2**) to maximize donor−metal bonding. The longer Sn···N interactions in **4** and **5** appear to result largely from tilting of the aromatic rings of the pyrimidine groups away from optimum bonding of the N centers (20.6−26.2° in **4** and 23.2−33.5° in **5**; cf. 2.9−9.8° in **2** and 2.5−13.2° in **3**), a situation which presumably stems from steric shielding of the donor N centers by the 4-Me groups in both complexes. This distortion can be seen most easily from the views of molecules of **2**, **3**, and **4** down their major axes, shown in Figure 5, illustrating the increasing tilting of the aromatic substituents brought about by increased substitution. In **6**, the large range of the intramolecular Sn···N interactions [2.838(5)−3.052(5) Å] is mirrored by the large range of deviations of the pyrimidine rings from the axes of the Sn···N contacts (9.9−25.2°). The shortest of these interactions [Sn(3)···N(8) 2.838(5) Å] is within the range of values found in **1** and **2**, while the remaining interactions are typical of those present in complexes **3**−**5** [3.030(5) Å and 3.052(5) Å]. The less regular pattern of the Sn···N interactions in **6** compared to those in **2**−**5** is most likely the consequence of increased steric crowding in the vicinity of the Sn^{IV} center, brought about by the presence of more sterically demanding MeO substituents. As noted earlier, the greater steric crowding within the ligand periphery of **6** is also suggested in the room-temperature ^{1}H NMR spectrum of the complex by the presence of two distinct resonances for the *endo*-4- and *exo*-6-MeO groups of the six 4,6-$(MeO)_2$pm ligands which span the two cubane subunits of the core. Closer inspection of the Sn−N bond lengths in **6** indicates that the greater steric demands of the 4,6-$(MeO)_2$pm ligands also result in significant distortions within the Sn_7N_8 core, and that the pattern of Sn···N interactions in the complex can be traced directly to these core distortions. Most notably, the weakness of the Sn(4)−N(7) bond [2.322(5) Å; cf. 2.198(5)−2.286(5) Å for the remaining Sn−N bonds in **6**] is compensated for by the particularly short Sn(3A)···N(8) interaction. Although there is some possibility of Sn···O bonding involving the 4-MeO substituents in **6** (the associated Sn···O distances [ca. 3.12−3.44 Å] being within the sum of the van der Waals radii of Sn and O [ca.3.70 Å] and similar to the intermolecular Sn···O interactions linking cubane molecules of $[Sn\{N(4\text{-}MeOC_6H_4)\}]_4$ and $[Sn\{N(3,4\text{-}(MeO)_2C_6H_3)\}]_4$ [3.303(6)−3.441(5) Å][7]), the orientation of the MeO groups in **5** *away* from the Sn···N interactions suggests that if present in **6** the intramolecular Sn···O interactions are extremely weak.

A further effect associated with increased substitution of the pyrimidine groups going from **2** to **3**−**6** is the modification of the *intermolecular* interactions. In **1**, where unsubstituted pyrimidine groups are present, the molecules are associated in the crystal lattice via intermolecular C−H···N hydrogen bonds [2.57 Å, C−H···N 177.9°] into a polymeric strand structure, in which the C−H at the 5-position of the pm groups attached to the symmetry-related N centers N(3) and N(3′) act as H-bond donors and two of the free pm N centers [N(6′) and N(6A)] act as H-bond acceptors (Figure

(24) Beswick, M. A.; Choi, N.; Harmer, C. N.; McPartlin, M.; Mosquera, M. E. G.; Raithby, P. R.; Tombul M.; Wright, D. S. *Chem. Commun. (Cambridge)* **1998**, 1383.
(25) Huheey, J. E. *Inorganic Chemistry*, 3rd ed.; Harper and Row: New York, 1993.

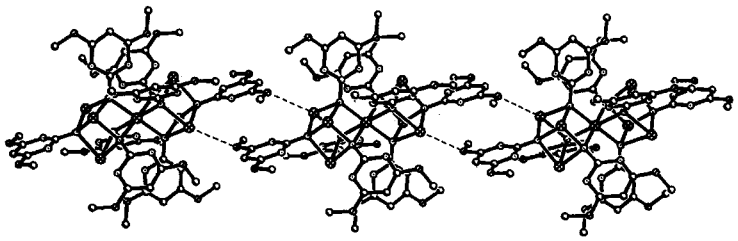

Figure 6. Packing of molecules of $[Sn_7\{2\text{-}N(pm)\}_8]\cdot 2thf$ (**2**) in the lattice, showing the propagation of the polymer via C−H···N interactions. Lattice-bound molecules of THF have been omitted for clarity.

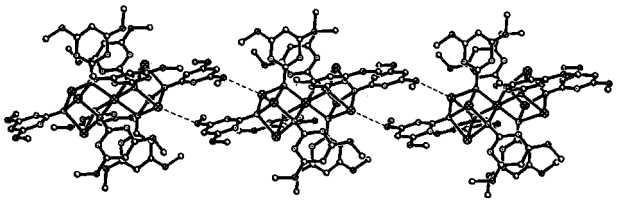

Figure 7. Packing of molecules of $[Sn_7\{2\text{-}N(4,6\text{-}(MeO)_2\text{-}Me_2pm)\}_8]$ (**6**) in the lattice, showing the propagation of the polymer via Sn···O interactions.

Table 3. B3LYP Energies for the Cubanes $[SnNR]_4$, Double-Cubane Counterparts $[Sn_7(NR)_8]$ [R = 2-(pm), Ph] and Other Reactant and Product Species

structure	SSD (au)[a]	SDB (au)[a]	SSD-L (au)[a,b]
$Sn(NMe_2)_2$	−272.49867	−272.55039	−272.57322
$PhNH_2$	−287.56516	−287.62270	
$(2\text{-pm})NH_2$	−319.63697	−319.71756	−319.74315
Me_2NH	−135.14211	−135.16647	−135.18350
Sn(0)	−3.33626	−3.34008	−3.33752
H_2	−1.17442	−1.17360	−1.17596
$[Sn\{2\text{-}N(pm)\}]_4$	−1287.47461	−1287.83182	−1287.89438
$[Sn\{N(Ph)\}]_4$	−1159.17227	−1159.42763	
$[Sn_7\{2\text{-}N(pm)\}_8]$	−2571.55349	−2572.26207	−2572.37983
$[Sn_7\{N(Ph)\}_8]$	−2314.87570	−2315.38644	

[a] 1 au = 627.5095 kcal/mol. [b] Geometry taken from SSD optimized structure.

6). As a result of steric congestion in the neighborhood of the corresponding C−H groups and N centers in **3**, **4**, and **5** which contain 4-Me, 4,6-Me, and 4-Me-6-MeO substitution, a similar pattern of association does not occur in their solid-state structures and no significant (directional) intermolecular interactions result. However, in **6** weak Sn···O interactions between one of the terminal MeO groups of the cage and one of the Sn centers of a neighboring molecule [Sn(4)··· O(23A) 3.569(6) Å] link the molecules into a polymeric arrangement, in a manner which is qualitatively similar to that found in **2** (Figure 7).

In order to investigate the importance of the interactions occurring in **1**−**6** as an influence on the double-cubane structure, a series of model DFT/B3LYP calculations were performed on the cubanes $[SnNPh]_4$ and $[Sn\{2\text{-}N(pm)\}]_4$ and the corresponding double cubanes $[Sn_7(NPh)_8]$ and $[Sn_7\{2\text{-}N(pm)\}_8]$. To evaluate the energetics of formation of the cubanes and double cubanes, calculations were also performed on the starting materials, $Sn(NMe_2)_2$, $PhNH_2$, $(2\text{-pm})NH_2$, and other potential products of the reactions, Sn, H_2, and Me_2NH. The energies of the geometry-optimized structures and single-point calculations are given in Table 3.

The optimized structure obtained from the B3LYP/SSD calculation of $[Sn_7\{2\text{-}N(pm)\}_8]$ (Figure 8) is similar to those of the structurally characterized complexes **1**−**6**. In particular,

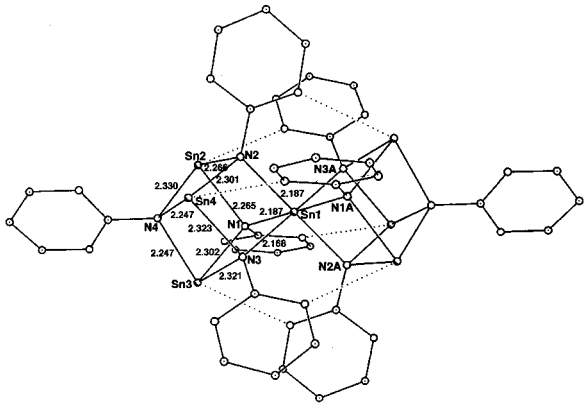

Figure 8. The optimized geometry for $[Sn_7\{2\text{-}N(pm)\}_8]$ at the B3LYP/SSD level.

the intramolecular Sn···N interactions which span the double cubane in the solid-state structure of $[Sn_7\{2\text{-}N(pm)\}_8]$ (**2**) [2.807(3)−2.935(3) Å] are very similar to those present in the calculated structure of the complex. Comparison of the optimized structures obtained from SSD and SDB calculations show that they are in close agreement, with bond lengths within 0.02 Å and angles within 2°. Examination of the calculated geometric parameters (based on the SDB optimized structure) versus those obtained experimentally reveals similar trends. The Sn(1)···N (cage) calculated distances are in the range 2.173−2.193 Å, differing from experiment by around 0.03 Å. In $[Sn_7\{2\text{-}N(pm)\}_8]$, Sn-(2,3,4)−N(1,2,3,4) calculated bond lengths are within a maximum difference of 0.04 Å compared to the experimental data. The internal angle within a cubane unit, N−Sn(1)−N, was found to be 81°, in close agreement with experiment (see Table 2) for $[Sn_7\{2\text{-}N(pm)\}_8]$. The internal cubane angles, N−Sn(2,3,4)−N, calculated for $[Sn_7\{2\text{-}N(pm)\}_8]$ have the values 76−80.1°, well within the experimental range given in Table 2. The calculated angles subtended between the cubane units in $[Sn_7\{2\text{-}N(pm)\}_8]$, designated by N−Sn-(1)−N, are in the range 99.1−99.2°, again in close agreement compared to the experimental data (see Table 2).

Comparison between the calculated SDB double-cubane structures, {$[Sn_7\{2\text{-}N(pm)\}_8]$ and $[Sn_7(NPh)_8]$}, reveals subtle but noticeable differences in bond lengths and angles. The Sn(1)−N bond lengths are in the range 2.282−2.293 Å for $[Sn_7(NPh)_8]$, significantly longer compared to the bond lengths in $[Sn_7\{2\text{-}N(pm)\}_8]$, while the calculated Sn(2,3,4)−N(1,2,3,4) bond distances are on average shorter, by 0.05 Å, in $[Sn_7(NPh)_8]$ than in $[Sn_7\{2\text{-}N(pm)\}_8]$. The internal angles, N−Sn(1)−N, in $[Sn_7(NPh)_8]$ are around 2.5° smaller compared to the same series of angles in $[Sn_7\{2\text{-}N(pm)\}_8]$.

In contrast, other internal angles within the cubane unit, N−Sn(2,3,4)−N, calculated for $[Sn_7(NPh)_8]$ are around 3−4° larger than those in $[Sn_7\{2\text{-}N(pm)\}_8]$. The angles subtended between the cubane units in $[Sn_7(NPh)_8]$, N−Sn(1)−N, are in the range 101.0−101.3°, which are larger than the corresponding angles in $[Sn_7\{2\text{-}N(pm)\}_8]$. A final structural distinction between the two calculated double-cubane structures involves the distance separating the terminal N atoms at either end of the double-cubane cage. In $[Sn_7(NPh)_8]$, the N···N separation is 7.978 Å, while in $[Sn_7\{2\text{-}N(pm)\}_8]$ this distance is 7.698 Å (cf. 7.559 Å in the solid-state structure of **2** and range 7.552−7.621 Å in **1**−**6**), revealing a more compact cage in the latter double cubane.

Scheme 2 summarizes reactions producing the cubanes $\{[Sn\{2\text{-}N(pm)\}]_4$ and $[Sn(NPh)]_4\}$ and double cubanes $\{[Sn_7\{2\text{-}N(pm)\}_8]$ and $[Sn_7(NPh)_8]\}$ from the reactants. The reaction which outlines the formation of the generic cubane structure is given in eq 1; the energy of formation of the cubane structures was calculated using this equation. For $[Sn\{2\text{-}N(pm)\}]_4$, the ΔE values were −43.3, −60.8, and −57.6 kcal mol^{-1} obtained from the SSD, SSD-L, and SDB calculations, respectively. The corresponding ΔE values for $[Sn(NPh)]_4$ were −42.1 and −33.8 kcal mol^{-1} extracted from the SSD and SDB calculations. It can be seen that the SSD, SSD-L, and SDB results are in qualitative agreement. We shall restrict future discussions of the energetics of reactions to the data taken from the SDB calculations. Equation 2 utilizes the same reactants but with a different stoichiometry to produce the double cubane. The resulting energies for the formation of $[Sn_7\{2\text{-}N(pm)\}_8]$ and $[Sn_7(NPh)_8]$ are −76.6 and −3.3 kcal mol^{-1}, respectively. Although the formation of the double cubane $[Sn_7\{2\text{-}N(pm)\}_8]$ is less favorable than that of its cubane counterpart based on reactant stoichiometry, significantly the formation of both is favorable. Switching the functional R group to phenyl has a dramatic effect on the formation of the double cubane based on the reactants common to both the single and double cubane. Although formation of the cubane $[Sn(NPh)]_4$ is highly favorable, the energetics in the formation of the double cubane $[Sn_7(NPh)_8]$ is now only slightly exothermic. As indicated by eq 3, it appears unlikely that the formation of the double cubanes occurs via disproportionation of the cubanes (as we had thought initially). The ΔE for the disproportionation of $[Sn\{2\text{-}N(pm)\}]_4$ to $[Sn_7\{2\text{-}N(pm)\}_8]$ is found to be +38.6 kcal mol^{-1}, and the corresponding reaction of $[Sn(NPh)]_4$ to $[Sn_7(NPh)_8]$ gives a ΔE of +80.8 kcal mol^{-1}. However, a promising alternative route in the formation of the double cubane may involve the interaction of the amine with the cubane to form the double cubane and hydrogen (eq 4). ΔE for the formation of $[Sn_7\{2\text{-}N(pm)\}_8]$ from the cubane and amine was calculated to be −31.2 kcal mol^{-1} whereas ΔE for $[Sn_7(NPh)_8]$ was +153.1 kcal mol^{-1}, a highly endothermic reaction. These results are in agreement with experimental findings, and so the next step is to combine eqs 1 and 4 to give an alternative reaction to eq 2 for the production of the double cubane from the reactants $Sn(NMe_2)_2$ and RNH_2, and this is presented in eq 5. The ΔE values for these

Scheme 2

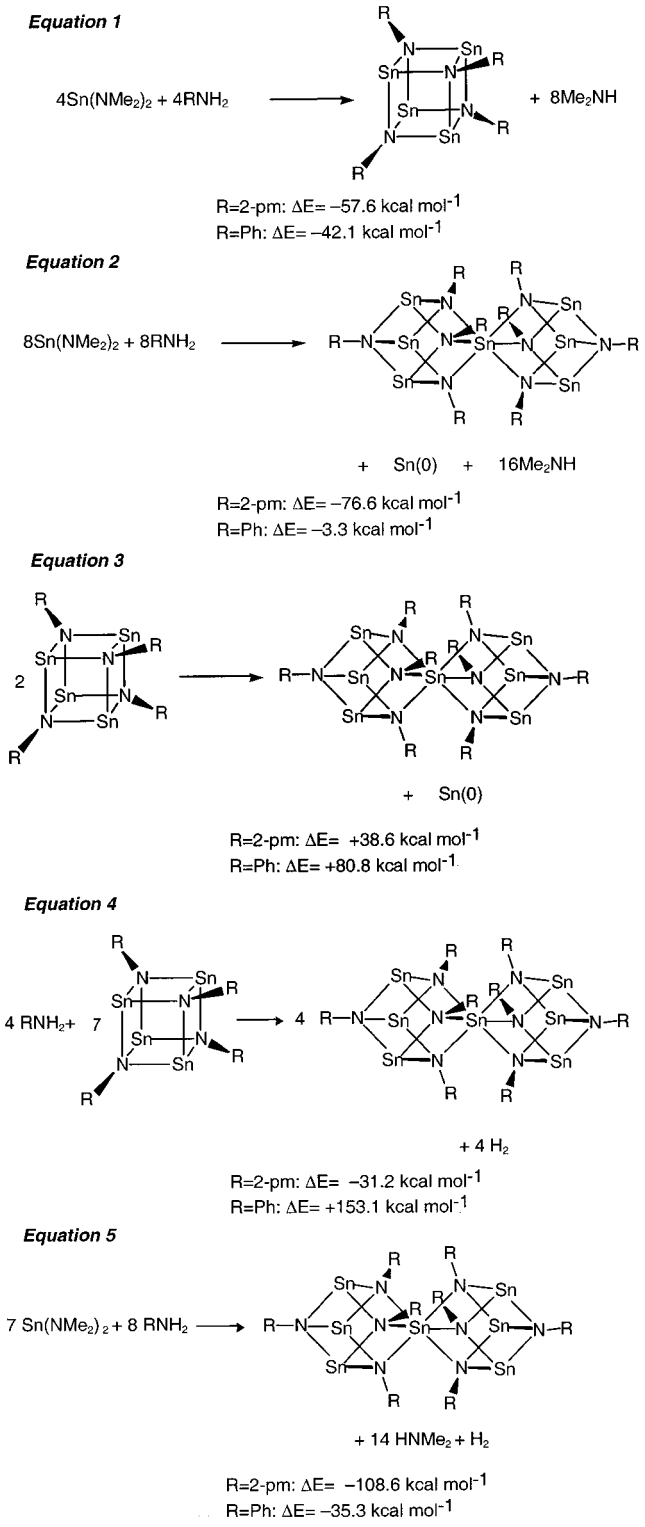

reactions are −108.6 and −35.3 kcal mol^{-1} for R = pm and Ph, respectively. A comparison of these results with the corresponding values for eq 1, taking into account the different stoichiometries of the reactants, leads to the conclusion that when the functional group (R) is pyrimidine the double-cubane structure is energetically preferred; however, when the R group is phenyl there is a predilection for the cubane geometry.

In an effort to rationalize the differing stabilities of $[Sn_7\{2\text{-}N(pm)\}_8]$ and $[Sn_7(NPh)_8]$ (the latter double cubane is not observed experimentally), an examination was undertaken of the charge distribution extracted from the calculations based on the B3LYP/SDB structures of the double cubanes. Analysis of the charge distribution within $[Sn_7\{2\text{-}N(pm)\}_8]$ reveals two distinct charged Sn elements within the cage structure. Sn(1) was assigned a charge of +1.489 and Sn(2,3,4) were assigned charges in the range +0.661 to +0.665. This is in qualitative agreement with experiment, namely, the charge on the central Sn atom is double that of the other Sn atoms within the double cubane. The nitrogen components within the cage are roughly equivalent and negatively charged, −0.718 to −0.737. These values should be compared to the single-cubane structure, $[Sn\{2\text{-}N(pm)\}]_4$, where all the Sn and N atoms are roughly equivalent in the cubane cage and are assigned charges, +0.689 and −0.724, respectively. In going from the cubane to the double-cube structure, the nitrogen (cage) charge remains fairly constant while the charge on the tin atoms increases by 0.02*e* except on the central tin atom where it decreases by 0.8*e*. The charge distribution observed within $[Sn_7(NPh)_8]$ is similar to that within $[Sn_7\{2\text{-}N(pm)\}_8]$, two distinct positively charged Sn moieties and roughly equivalent negatively charged nitrogen (cage) elements. For Sn(1) the charge assigned was +1.277 while the remainder of the Sn atoms fell in the range +0.544 to +0.560. Thus, there is less positive charge on the Sn elements compared to the same components in $[Sn_7\{2\text{-}N(pm)\}_8]$. For the nitrogen atoms within the double-cubane cage of $[Sn_7(NPh)_8]$, the charges assigned were in the range −0.723 to −0.732, close to the range of the same elements in $[Sn_7\{2\text{-}N(pm)\}_8]$. In $[Sn(NPh)]_4$ the formal charges for Sn and N were assigned the values of +0.609 and −0.741, respectively.

In $[Sn_7\{2\text{-}N(pm)\}_8]$, there is the potential for six cross-linkages between Sn [omitting Sn(1)] and N in 2-pm [omitting the two terminal 2-pm rings]. If there is an interaction between these elements, there should be a charge difference between the two nitrogens contained in the 2-pm ring. Charge analysis reveals a significant difference in the charge residing on the nitrogens in the 2-pm ring. The nitrogen (2-pm) facing the Sn, on the opposite cubane, has a net charge in the range −0.245 to −0.259, while the nitrogen farthest away on the 2-pm ring has a charge of −0.221 to −0.227. These values should be compared to the single-cubane charges on nitrogen contained in the 2-pm ring of −0.214 to −0.220. The nitrogen (2-pm ring) facing the Sn has gained negative charge, in the range 0.02−0.03*e*, while the other nitrogen contained in the 2-pm structure remains unchanged in going from the cubane to the double-cubane structure. The cross-linkage separation for the Sn···N electrostatic interaction falls in the range 2.97−3.05 Å in $[Sn_7\{2\text{-}N(pm)\}_8]$. In the $[Sn_7(NPh)_8]$ structure, there are no significant changes in the charge distribution on the phenyl group in going from the cubane to the double cubane. There are no Sn−phenyl cross-linkage separations in the range 2.97−3.05 Å found in $[Sn_7(NPh)_8]$, and thus no significant cross-linkage electrostatic interaction could be manifest within this double-cubane entity. Figure 9 depicts isosurface electrostatic potentials for $[Sn_7\{2\text{-}N(pm)\}_8]$ and $[Sn_7(NPh)_8]$. There are clear differences in charge distribution within these double cubanes. The orientations of both double cubanes are similar, a side view with both end R groups clearly visible. In Figure 9a, $[Sn_7\{2\text{-}N(pm)\}_8]$, in the foreground, the top ring (2-pm) is viewed to be interacting with the Sn to the left while the bottom ring (2-pm) is viewed to be interacting with the Sn to the right. Both these interactions are electrostatic in nature and utilize components from the opposite cubane in the double-cubane structure. These interactions are not evident in Figure 9b on the $[Sn_7(NPh)_8]$ isosurface. The R group plays an important role in determining whether or not these cross-linkage interactions can take place and in essence plays a role in the stability (or lack thereof) in the double cubane.

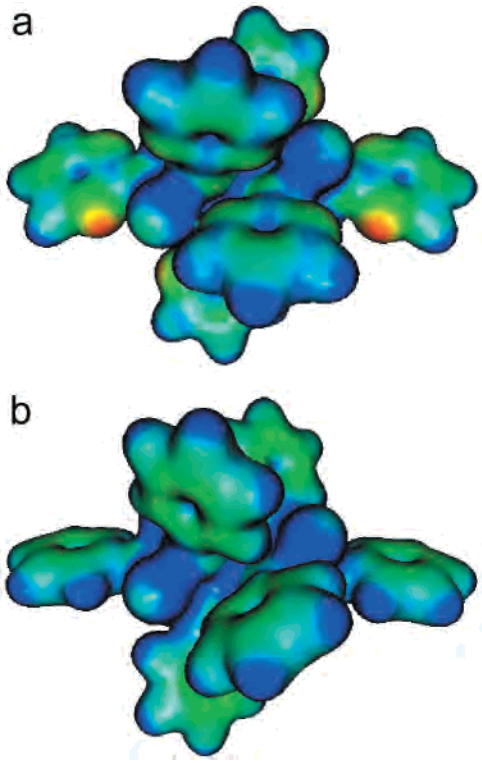

Figure 9. Isodensity surface of the electrostatic potential for (a) $[Sn_7\{2\text{-}N(pm)\}_8]$ and (b) $[Sn_7(NPh)_8]$. Color: (most negative charge) red < yellow < green < light blue < blue (most positive charge).

Conclusions

The study of the reactions of $Sn(NMe_2)_2$ with various functionalized primary amines (RNH_2) presented in this paper illustrates that the nature and structure of the imido complexes produced is dependent on the characteristics of the organic substituents (R). Where pyridine or pyrimidine functionality is present, the possibilty of intramolecular N···Sn interactions has a major effect in directing the formation of mixed-oxidation-state double cubanes of the type $[Sn_7(NR)_8]$. Theoretical calculations suggest that the formation of the double-cubane structures does not arise from disproportionation of two cubane precursors (as was originally proposed). A more likely scenario involves the production of molecular H_2. This suggestion provides some interesting

prospects for future studies. In particular, it may be possible to effect selective aggregation of cubanes or even double cubanes by their interaction with pyridyl or pyrimidyl amines.

Acknowledgment. We gratefully acknowledge the EPSRC (A.D.B., N.F., E.A.H., M.M.), Churchill and Fitzwilliam Colleges (A.D.H.), the EU (fellowship for E.A.Q., Socrates grant for D.S. [Cambridge (U.K.)/Oviedo (Spain)]), and the Leverhulme Trust (D.S.W.) for financial support. D.M. acknowledges the support of the Office of Energy Research, Office of Basic Energy Sciences, Division of Chemical Sciences, U.S. Department of Energy under Grant DE-FG02-97ER-14758. We also thank Dr. J. E. Davies for collecting X-ray data on **1**−**5**.

Supporting Information Available: Crystallographic data available (CIF) for structures **3**, **4**, **5**, and **6**. This material is available free of charge via the Internet at http://pubs.acs.org.

IC011090R